

Geometry of Reaction Interfaces in Chaotic Flows

M. Giona,* S. Cerbelli, and A. Adrover

Dipartimento di Ingegneria Chimica, Centro Interuniversitario sui Sistemi Disordinati e sui Frattali nell'Ingegneria Chimica, Università di Roma "La Sapienza," via Eudossiana 18, 00184 Roma, Italy

(Received 21 March 2001; published 27 December 2001)

The analysis of transport-controlled reactions in chaotic flows provides a physical frame to extend the concept of the intermaterial contact area (ICA)—introduced in the purely kinematic case—to mixing systems with diffusion, where the ICA is identified through the reaction interface between segregated reactants. We show that the dynamics of the ICA undergoes a crossover from kinematics-dominated exponential growth to a persistent oscillatory regime resulting from the intertwined action of advection and diffusion. The scaling of the crossover length versus the Peclet number is analyzed.

DOI: 10.1103/PhysRevLett.88.024501

PACS numbers: 47.70.Fw, 05.45.-a, 47.52.+j, 47.54.+r

The response of a physical process occurring in a stirred fluid system depends significantly upon the interaction between diffusion and convective stirring. Well-known examples include heat and mass transport with or without chemical reactions [1,2] as well as the growth of magnetic-field seeds in chaotic flows (the so-called *fast dynamo* problem) [3]. Several different approaches have been used to describe and quantify the interplay between stirring effects induced by a chaotic flow and diffusion: statistical analysis of mean square displacement [4]; methods based on Melnikov theorem [5] and shadowing techniques [6]; time splitting between diffusion and convection (*pulsed systems*) [3,7]; analysis of diffusing-reacting systems for which the nonlocal effects of diffusion can be neglected [8]; analysis of premixed lamellar systems under diffusion [9,10]; numerical simulations of advecting-diffusing-reacting systems [11].

There is, however, one important feature that has not been addressed: namely, the question of how the geometry of partially mixed structures—with specific reference to the dynamics of interfaces undergoing chaotic advection—is modified by molecular diffusion. Besides, the knowledge of pattern dynamics, under stirring, diffusion, and, possibly, chemical reactions, provides important phenomenological information useful to build up models of industrial reacting flows [1], dispersion of solid and liquid pollutants, growth of microorganisms in flowing media [12], etc.

The natural physical framework to approach the dynamics of segregation patterns is given by transport-controlled [13] bimolecular chemical reactions $A + B \rightarrow P$, on the assumption of equal molecular diffusivity and stoichiometric loading of the reactants [10]. Beyond its practical relevance (mixing-controlled reactions), the assumption of transport-controlled kinetics is crucial in that it implies that the species A and B remain segregated at all times, as they cannot coexist at one and the same spatial location. The ICA can therefore be identified as the *reaction interface* between the two segregated reactants, and the system considered provides a simple physical framework for a well-posed comparison between the evolution of

partially mixed structures with and without molecular diffusion [14].

This Letter analyzes the geometry and dynamics of reaction interfaces and of the corresponding mixing patterns for transport-controlled reactions in chaotic flows in the presence of diffusion.

In quantitative terms, the evolution of the system is described by the single partial differential equation [9,10]:

$$\frac{\partial \phi}{\partial t} + \mathbf{v}(\mathbf{x}, t) \cdot \nabla \phi = \frac{1}{\text{Pe}} \Delta \phi, \quad (1)$$

defined on a differentiable manifold \mathcal{M} representing the mixing space, where $\phi = C_A - C_B$, Pe is the Peclet number, $\text{Pe} = VL/\mathcal{D}$, V , L being characteristic velocity and length of the system. While two-dimensional time-periodic velocity fields $\mathbf{v}(\mathbf{x}, t)$ are considered throughout this Letter, all of the results can be straightforwardly extended to three-dimensional systems.

The stoichiometric loading of reactants implies $m_A(0) = \int_{\mathcal{M}} C_A(\mathbf{x}, 0) d\mathbf{x} = m_B(0) = \int_{\mathcal{M}} C_B(\mathbf{x}, 0) d\mathbf{x}$, where $C_\alpha(\mathbf{x}, 0)$ is the initial concentration of the species α , and $\mathbf{x} = (x, y)$.

At all positive times, the solution of Eq. (1) is smooth, and the boundary between the segregated reactants (i.e., the reaction interface) coincides with zero level set $\gamma(t) = \{\mathbf{x} \in \mathcal{M} | \phi(\mathbf{x}, t) = \langle \phi(\mathbf{x}, t) \rangle = \int_{\mathcal{M}} \phi(\mathbf{x}, 0) d\mathbf{x}\}$, where $\langle \phi(\mathbf{x}, t) \rangle = 0$ by virtue of the initial condition.

Although motivated by the physical system described above, the level set $\gamma(t)$ can be regarded in a more general sense as a well-defined feature associated with the partial differential equation [Eq. (1)] whenever the initial distribution $\phi(\mathbf{x}, 0)$ is nonconstant.

As a model system, we consider a two-dimensional time-periodic flow (sine flow [15]) obtained by blinking every $T/2$ time units the two steady fields $\mathbf{v}_1 = [\sin(2\pi y), 0]$ and $\mathbf{v}_2 = [0, \sin(2\pi x)]$ defined on the two-dimensional torus (i.e., on the unit square $\mathcal{M} = I^2$ equipped with periodic boundary conditions). The initial condition is set to $\phi(\mathbf{x}, 0) = 2 - 4\eta(x - 1/2)$, where $\eta(x)$ is the unit step function, corresponding to a unit initial mass of the reactants, each occupying half of the

unit square I^2 . The kinematic interface in the limit $Pe = \infty$ is obtained by advecting the segments $x = 0$ and $x = 1/2$ (which constitute the intermaterial boundary at $t = 0$) through the ordinary differential equation (ODE) $\dot{\mathbf{x}} = \mathbf{v}(\mathbf{x}, t)$.

Expansion of the function ϕ in Fourier series, $\phi(\mathbf{x}, t) = \sum_{h,k=-\infty}^{\infty} \phi_{h,k}(t) \exp[2\pi i(hx + ky)]$, and substitution into Eq. (1) yields the following infinite-dimensional linear tridiagonal system of ODEs for the coefficients during the first half-period $T/2$ (motion along the x axis):

$$\dot{\phi}_{h,k} = -\frac{4\pi^2}{Pe} (h^2 + k^2) \phi_{h,k} - \pi h (\phi_{h,k-1} - \phi_{h,k+1}). \quad (2)$$

An analogous equation is obtained for the other half-period by interchanging h and k .

Equation (2) was solved numerically for $10^2 \leq Pe \leq 10^5$ with $h, k \in -N, \dots, N$, where N [the number of modes is $(2N + 1)^2$] varied from 80 (for the lowest Pe) to 300 (for $Pe = 10^5$). The number of modes was chosen so as to ensure N independence of the solution in the norm L^2 . In order to determine both the spatial patterns and the overall interface length, the values of ϕ on a square mesh of 512×512 nodes were computed by means of a standard fast Fourier transform algorithm. The nodal values of function ϕ were linearly interpolated and the reaction interface $\gamma(t)$ was determined as the intersection of the globally continuous piecewise triangular surface with the plane $\phi = 0$. The mesh utilized proved fine enough to resolve the details of mixing patterns for all of the finite Pe values considered.

Interface tracking for the $Pe = \infty$ case was accomplished by advecting interface points through the first-order ODE $\dot{\mathbf{x}} = \mathbf{v}(\mathbf{x}, t)$.

Figures 1(a)–1(d) show the segregation patterns (white and gray) and the reaction interface γ (black line) for a mixing protocol specified by a period $T = 1.6$ at $Pe = 10^4$ at times nT , with $n = 1, 2, 3$, and 5, respectively. In the same figure, the structure of the kinematic interface ($Pe = \infty$) is shown at the end of the first (I) and second (II) periods. It is worth noting that the value $T = 1.6$ of the switching period yields a nearly globally chaotic protocol. In this situation, the stroboscopic evolution of the kinematic interface undergoes invariant space-filling exponential growth, as can be observed from (I) and (II) in Fig. 1. Snapshots of the kinematic interface at later times (not shown here for the sake of brevity) yield what is essentially the same structure supplemented with increasingly fine detail.

Comparison of Fig. 1(a) and (I) shows that at the end of the first period the reaction interface is indistinguishable from the corresponding kinematic ($Pe = \infty$) interface. The situation changes drastically at the end of the second period, as can be observed by comparing Fig. 1(b) and (II). Diffusion swiftly merged and erased many of the fine scale

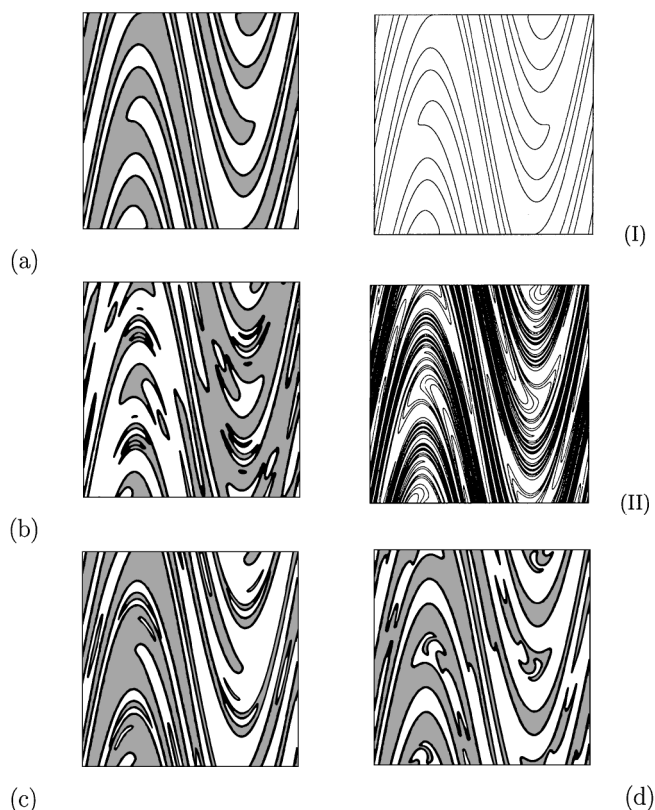


FIG. 1. Comparison of the kinematic ($Pe = \infty$) and reaction interfaces at $Pe = 10^4$ for the globally chaotic protocol $T = 1.6$. (a)–(d) Mixing patterns (white and gray) and reaction interface (black line) at times $T, 2T, 3T$, and $5T$ in sine flow for $T = 1.6$ (globally chaotic case). (I), (II) Kinematic interface at the end of the first (I) and second (II) periods.

structures, causing an enormous reduction of the overall interface length. The patterns corresponding to the third and the fifth period [Figs. 1(c) and 1(d)] show the attainment of a type of persistent oscillatory behavior in the geometry of the structures. These oscillatory patterns can be seen qualitatively as the resultant of a dynamical equilibrium between two competing mechanisms, namely, the convection-driven generation of the interface and the merging of neighboring structures due to molecular diffusion [16].

An important question arises as to the role of chaos in determining the dynamics of reaction interfaces. In order to explore this point, we analyzed the case of a stirring protocol that possesses large regions of regular motion (islands), as can be obtained, for example, by setting the periodicity of the sine flow system to the value $T = 0.4$. Figure 2-(I) and 2-(II) show the snapshots of the kinematic ($Pe = \infty$) interface at times nT , with $n = 20$ and $n = 30$, respectively. In this case, the material interface undergoes altogether different stretching processes inside and outside the chaotic region, the overall rate of growth being exponential in the chaotic region (X -shaped area in the figures) and linear within the islands. The corresponding reaction interfaces at $Pe = 10^4$ [Figs. 2(a) and 2(b)] coincide with the kinematic template within the islands, while the fine

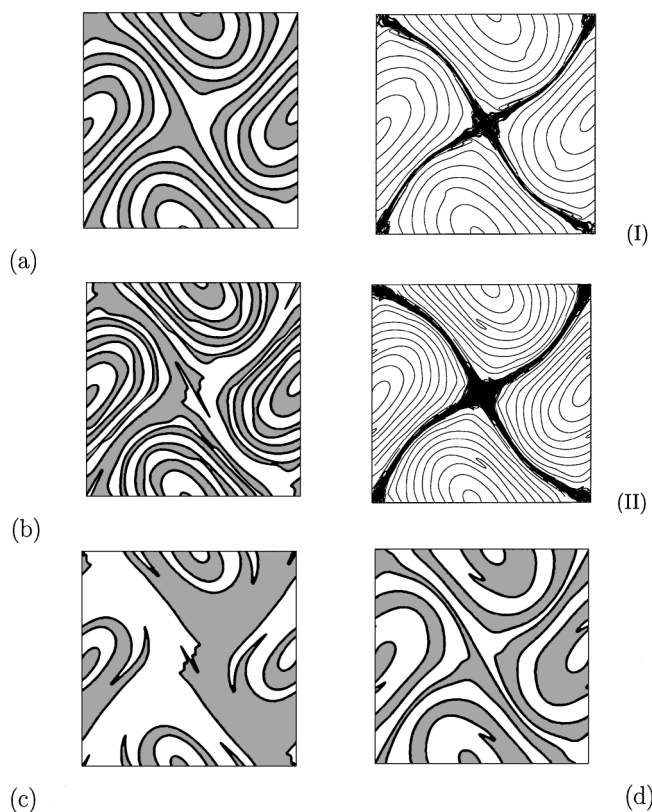


FIG. 2. Comparison of the kinematic ($Pe = \infty$) and reaction interfaces at $Pe = 10^4$ for a mixing protocol with large quasiperiodic islands ($T = 0.4$). (a)–(d) Mixing patterns (white and gray) and reaction interface (black line) at times $20T$, $30T$, $50T$, and $60T$. (I), (II) Kinematic interface at time $20T$ (I) and $30T$ (II).

structure of the diffusionless limit inside the chaotic region is evidently blurred into one large lamella at the times considered. Snapshots of the reactive patterns at later times [$n = 50$, Fig. 2(c); and $n = 60$, Fig. 2(d)] again point to a persistent oscillatory evolution in the mixing patterns. All of these qualitative observations find a simple and rigorous explanation in the analysis of Eq. (1) regarded as a dynamical system in a functional space [17].

An overall quantitative description of interface dynamics can be obtained by tracking the length of the reaction interface $L(t)$ vs time. We consider a wide range of $Pe = 10^2 \div 10^5$ for the two mixing protocols ($T = 0.4$ and $T = 1.6$). Figure 3(a) shows the results for the nearly globally chaotic case $T = 1.6$, at $Pe = 10^3, 10^4$, and 10^5 (continuous lines), together with the growth of the kinematic interface (line with points). For each of the Pe considered, we can unambiguously identify a crossover time $t^* = t^*(Pe)$ (and a corresponding breakup length L^*) beyond which the dynamics of reaction interfaces departs irreversibly from exponential kinematic growth and settles into a bounded oscillating pattern around a characteristic average length depending on Pe and on the mixing protocol.

The case $T = 0.4$ [Fig. 3(b)] displays more complex features. Here it is possible to identify two separate

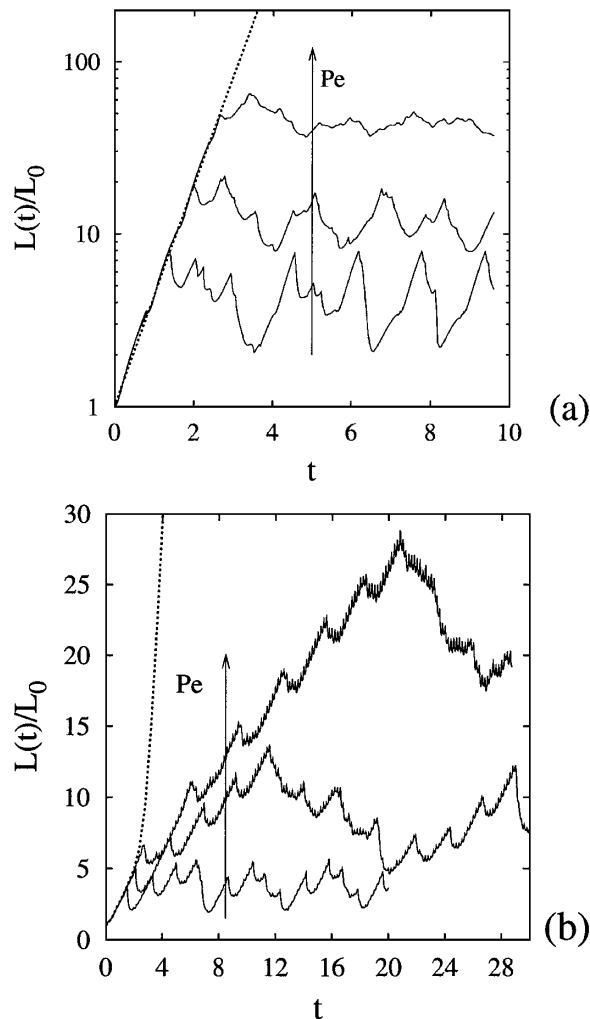


FIG. 3. Length of the reaction interface $L(t)$ vs time for sine flow at $T = 1.6$ (a) and $T = 0.4$ (b). Continuous lines: $Pe = 10^3, 10^4, 10^5$. Dotted line: kinematic interface.

crossover times t_C^* and t_P^* corresponding, respectively, to the breakup of the kinematic interface inside and outside the chaotic region. For $t_C^* < t < t_P^*$, the interface undergoes an oscillating restructuring driven by repeated merging events inside the chaotic region, whereas the overall trend of monotonic growth is driven by the fraction of interface that falls within the islands. If we target the $Pe = 10^4$ case (second curve from below), the breakup time t_P^* proves to be in the order of $t_P^* = 11.6$, which corresponds to approximately $n = 28$ periods, while $t_C^* = 2.1$. Comparison of the kinematic and reaction interfaces at $n = 30$ ($t = 12$) [Fig. 1(b) and Fig. 1-(II)] supports the observation that significant merging of structures within the islands begins only at times larger than $t_P^* = 11.6$. The small high-frequency fluctuations (in the time scale of a half-period) clearly detectable for $T = 0.4$, and especially at high Peclet numbers, are not spurious consequences of the numerics, but rather of merging and restructuring events between parts of the interface that lie “at the border” between the quasiperiodic and chaotic regions.

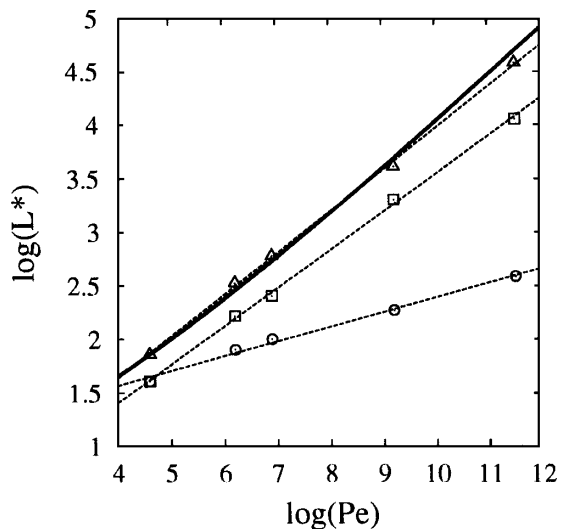


FIG. 4. Scaling of breakup length $L^*(t_C^*)$ vs Pe for sine flow. (Δ): $T = 1.6$; (\circ): $T = 0.4$. The continuous line represents the prediction of $L^* = L^*(Pe)$ derived from scaling arguments (see main text) for the case $T = 1.6$. The boxes (\square) represent $L^*(t_p^*)$ at $T = 0.4$.

It is worth pointing out that the breakup time t^* does not correspond to the extinction of the reaction. Indeed, taking the $T = 1.6$ case as an example, $m_A(t^*) = 0.40, 0.56$, and 0.66 for $Pe = 10^3, 10^4$, and 10^5 , respectively. As regards the kinetics of reactant consumption, this means that for high Peclet numbers the major contribution to reaction occurs in the mixed regime ($t > t^*$) rather than in the kinematic-controlled regime ($t < t^*$). Moreover, in the mixed regime, the partially mixed structures attain an almost constant average thickness approximately equal to $1/L^*$.

Figure 4 shows the scaling of the breakup length L^* vs the Peclet number for both $T = 0.4$ and $T = 1.6$. In the first case, both $L(t_C^*)$ and $L(t_p^*)$ are shown. In all of the cases examined, $L^* \sim Pe^\nu$ over three decades, where $\nu = 1/8$ for $L(t_C^*)$, $\nu = 1/3$ for $L(t_p^*)$, and $\nu = 0.4$ for L^* at $T = 1.6$. Focusing attention on the nearly globally chaotic case, the behavior of L^* vs Pe can be explained by means of elementary scaling arguments. The first breakup of the reaction interface, which coincides with the kinematic interface up to that time, occurs when the diffusional length scale $l_{\text{diff}} = (2t/Pe)^{1/2}$ is of the same order of magnitude as the average lamellar thickness $1/L_{\text{kin}}(t)$, i.e., $l_{\text{diff}}(t^*) = \alpha L_{\text{kin}}^{-1}(t^*)$, the prefactor $\alpha \sim O(1)$ accounting for the spatial heterogeneity of the short-time Lyapunov exponents, which determines the fine structure of the local striation thickness and can be estimated from a single simulation experiment at low $Pe = 10^2$. The length of the kinematic interface is given by $L_{\text{kin}}(t) = L_0 \exp(h_{\text{top}} t/T)$, $L_0 = 2$, where h_{top} is the topological entropy of the system estimated from its Poincaré map ($h_{\text{top}} = 2.33$ for $T = 1.6$). t^* is therefore implicitly expressed by the equation $Pe = 8\alpha^2 t^* \exp(2\theta t^*/T)$, with $\alpha = 0.62$ for $T = 1.6$.

The geometric approach undertaken in this Letter can be also exploited to predict overall reactant decay through one-dimensional models [17].

*Author to whom correspondence should be addressed.

- [1] J. Baldyga and J. R. Bourne, *Turbulent Mixing and Chemical Reactions* (Wiley, New York, 1999).
- [2] A. Mokrani, C. Catelain, and H. Peerhossaini, *Int. J. Heat Mass Transf.* **40**, 3089 (1997); D. R. Sawyers, M. Sen, and H.-C. Chang, *Int. J. Heat Mass Transf.* **41**, 3559 (1998).
- [3] S. Childress and A. D. Gilbert, *Stretch, Twist, Fold: The Fast Dynamo* (Springer Verlag, Berlin, 1995); V. I. Arnold and B. A. Khesin, *Topological Methods in Hydrodynamics* (Springer-Verlag, Berlin, 1998).
- [4] S. W. Jones, *Phys. Fluids A* **3**, 1081 (1991); S. Benkadda, S. Kassibrakis, R. B. White, and G. M. Zaslavsky, *Phys. Rev. E* **55**, 4909 (1997); M. Clück, A. R. Kolovsky, and H. J. Korsch, *Physica (Amsterdam)* **116D**, 283 (1998).
- [5] V. Rom-Kedar and A. C. Poje, *Phys. Fluids* **11**, 2044 (1999).
- [6] I. Klapper, *Phys. Fluids A* **4**, 861 (1992).
- [7] J. M. Finn and E. Ott, *Phys. Fluids B* **2**, 916 (1990).
- [8] Z. Neufeld, C. Lopez, and P. H. Haynes, *Phys. Rev. Lett.* **82**, 2606 (1999); T. Tel, G. Karolyi, A. Pentek, I. Scheuring, Z. Toroczkai, C. Grebogi, and J. Kadtke, *Chaos* **10**, 89 (2000); C. Lopez, E. Hernandez-Garcia, O. Piro, A. Vulpiani, and E. Zambianchi, *Chaos* **11**, 397 (2001).
- [9] R. Chella and J. M. Ottino, *Chem. Eng. Sci.* **39**, 551 (1983); I. M. Sokolov and A. Blumen, *Phys. Rev. A* **43**, 2714 (1991); **43**, 6545 (1991).
- [10] F. J. Muzzio and J. M. Ottino, *Phys. Rev. Lett.* **63**, 47 (1989); I. M. Sokolov and A. Blumen, *Int. J. Mod. Phys. B* **20**, 3127 (1991).
- [11] F. J. Muzzio and M. Liu, *Chem. Eng. J.* **64**, 117 (1996); R. Reigada, F. Sagues, I. M. Sokolov, J. M. Sancho, and A. Blumen, *J. Chem. Phys.* **107**, 843 (1997); J. M. Zalc and F. J. Muzzio, *Chem. Eng. Sci.* **54**, 1053 (1999).
- [12] I. R. Epstein, *Nature (London)*, **374**, 321 (1995).
- [13] In chemical reaction kinetics, the wording "transport-controlled reaction" is usually referred to as *infinitely fast* or *instantaneous* reactions.
- [14] See, e.g., D. Beigie, A. Leonard, and S. Wiggins, *Chaos Solitons Fractals* **4**, 749 (1994); V. Rom-Kedar, A. Leonard, and S. Wiggins, *J. Fluid Mech.* **214**, 347 (1991); M. M. Alvarez, F. J. Muzzio, S. Cerbelli, A. Adrover, and M. Giona, *Phys. Rev. Lett.* **81**, 3395 (1998); M. Giona and A. Adrover, *Phys. Rev. Lett.* **81**, 3864 (1998).
- [15] M. Liu, F. J. Muzzio, and R. L. Peskin, *Chaos Solitons Fractals* **4**, 869 (1994).
- [16] X. Z. Tang and A. H. Boozer, *Physica (Amsterdam)* **95D**, 283 (1996).
- [17] See AIP Document No. EPAPS: E-PRLTAO-88-006202 for an analysis of Eq. (1); understanding stationary dynamics of reaction interface and predicting overall reaction rates. This document may be retrieved via the EPAPS homepage (<http://www.aip.org/pubservs/epaps.html>) or from <ftp.aip.org> in the directory `/epaps/`. See the EPAPS homepage for more information.